Indiana University - Bloomington

Discovering New Particles at Colliders

M.S. Berger[1] and W. Merritt[2]

[1] *Physics Department, Indiana University, Bloomington, IN 47405, USA*
[2] *Fermi National Accelerator Laboratory, Batavia, IL 60510, USA*

Abstract

We summarize the activities of the New Particles Subgroup at the 1996 Snowmass Workshop. We present the expectations for discovery or exclusion of leptoquarks at hadron and lepton colliders in the pair production and single production modes. The indirect detection of a scalar lepton quark at polarized e^+e^- and $\mu^+\mu^-$ colliders is discussed. The discovery prospects for particles with two units of lepton number is discussed. We summarize the analysis of the single production of neutral heavy leptons at lepton colliders.

1   Introduction

With the recent discovery of a new particle at the Tevatron, one of the last holes in the Standard Model has been filled. Only the elusive Higgs boson remains undetected, and the next new particle discovery may usher in a revolution in our understanding. The area covered by the subgroup was all new particles which are fundamental and not covered by other groups at Snowmass. This includes fermions with exotic (non-Standard Model) quantum numbers, sequential fermions (i.e. a fourth generation), and leptoquarks and diquarks. Other new particles covered by other working groups such as the Higgs boson and supersymmetric particles were omitted from our studies. New non-fundamental (composite) particles such as excited fermions and technipions were relegated to the New Interactions subgroup[1]. A recent review of new particles and interactions can be found in Ref. [2].

In this report we summarize the individual contributions to the New Particles subgroup. For more details the individual contributions should be consulted.

2   Leptoquarks

Theories attempting to unify the leptons and quarks in some common framework often contain new states that couple to lepton-quark pairs, and hence are called leptoquarks[3]. Necessarily leptoquarks are color triplets, carry both baryon number and lepton number, and can be either spin-0 (scalar) or spin-1 (vector) particles. Perhaps the most well-known examples of leptoquarks appear as gauge bosons of grand unified theories[4]. To prevent rapid proton decay they must be very heavy and unobservable, or their couplings must be constrained by symmetries. Nonetheless, much work has been devoted to signals for the detection of leptoquarks at present and future colliders[5, 6, 7, 8, 9, 10]. Searches have already been performed at LEP[11], HERA[12], and the Tevatron[13]. One potentially attractive source of light leptoquarks is in E_6 models where the scalar leptoquark can arise as the supersymmetric partner to the color-triplet quark that naturally resides in the fundamental representation **27**. A recent review of the physics signals for leptoquarks can be found in Ref. [2].

Leptoquarks can be sought by looking for indirect effects in low energy processes[14]. Light leptoquarks (less than a several hundred GeV) must also satisfy strong con-

straints from flavor changing neutral current processes, so that leptoquarks must couple to a single generation of quarks and leptons. The most convincing evidence for leptoquarks would come from their direct production and detection at colliders. For the heavy leptoquarks that might be detected at the multi-TeV machines, the constraints from low energy processes do not necessarily require this, since the leptoquark's virtual contributions are suppressed by its large mass.

Various methods have been proposed to search for leptoquarks. At lepton colliders (e^+e^- and $\mu^+\mu^-$) colliders, leptoquarks can be produced in pairs via s-channel γ and Z exchange, and by t-channel exchange of a quark. The coupling of a leptoquark is not constained by the usual gauge symmetries (it is a Yukawa coupling), so there is some model dependence that necessarily enters in some cross section calculations. The production cross section depends sensitively on the leptoquark couplings so that the constraints depend on its quantum numbers.

Leptoquarks decay into a lepton and a quark, giving quite distinctive signals. The signatures for leptoquark pair production are therefore: (1) two charged leptons and two hadronic jets, (2) one charged lepton, two hadronic jets and missing energy (neutrino), and (3) two hadronic jets and missing energy. For relatively light leptoquarks, the constraints from flavor-changing neutral currents generally constrain the leptoquark couplings to be within a single generation so that the leptons in the final state will be in the same family. For heavier leptoquarks ($M_{LQ} > 1$ TeV) this is not necessarily the case and more exotic final states are possible.

Single production of leptoquarks is also possible. The cross sections for these processes generally depend on the unknown Yukawa coupling. The advantage in this case is that one can obtain a higher reach in leptoquark mass since kinematically one only needs center-of-mass energy to make one heavy particle.

Finally, one can look for virtual effects of leptoquarks (zero-production of leptoquarks). In this case one can exclude leptoquarks in excess of the colliders center-of-mass energy by looking for deviations from the Standard Model predictions for cross sections and asymmetries.

3   Pair Production of Leptoquarks in Hadron SuperColliders

Rizzo[15] examined the search reach for both scalar and vector leptoquarks at future hadron supercolliders. The colliders considered are the $\sqrt{s}$=60 (LSGNA) and 200 (PIPETRON) TeV machines, operating in either a pp or $p\bar{p}$ mode. At these energies and the anticipated luminosities leptoquarks even above a TeV are accessible.

The dominant production for leptoquarks at a hadron collider is expected to be pair production, which proceeds through QCD interactions (in either gg or $q\bar{q}$ collisions) and depends only on the leptoquark spin and the fact that it is a color triplet field[16].

For vector leptoquarks (V), one can assume that they are the gauge bosons of an extended gauge group. Then the gVV and $ggVV$ couplings are fixed by extended gauge invariance. The Feynman rules needed for calculating the production cross section can then be derived from the following Lagrangian[17]

$$\mathcal{L}_V = -\frac{1}{2}F_{\mu\nu}^{\dagger}F^{\mu\nu} + M_V^2 V_{\mu}^{\dagger}V^{\mu} - ig_s V_{\mu}^{\dagger}G^{\mu\nu}V_{\nu}\,. \tag{1}$$

Here, $G_{\mu\nu}$ is the usual gluon field strength tensor, V_{μ} is the vector leptoquark field and $F_{\mu\nu} = D_{\mu}V_{\nu} - D_{\nu}V_{\mu}$, where $D_{\mu} = \partial_{\mu} + ig_s T^a G_{\mu}^a$ is the gauge covariant derivative (with respect to $SU(3)$ color), G_{μ}^a is the gluon field and the $SU(3)$ generator T^a is taken in the triplet representation. One can be more general than this i.e. not necessarily assuming that the leptoquark is a fundamental gauge boson. Then one can introduce an undetermined parameter κ in the last term that acts as an anomalous chromomagnetic moment; see Ref. [15] for details.

The cross sections for S and V pair production at the $\sqrt{s}$=60 (LSGNA) and 200 (PIPETRON) TeV machines are displayed in Figures 1, 2, 3 and 4. The corresponding results for the Tevatron and LHC have been presented previously in, e.g., Ref.[2]. The contributions of the subprocesses $gg \rightarrow SS, VV$ and $q\bar{q} \rightarrow SS, VV$ are displayed along with the total cross section. The following conclusions can be drawn[15]:

- The vector leptoquark cross section is substantially larger than that for scalars in both pp and $p\bar{p}$ collisions since the rates for both $gg \rightarrow VV$ and $q\bar{q} \rightarrow VV$ are larger than their scalar counterparts.
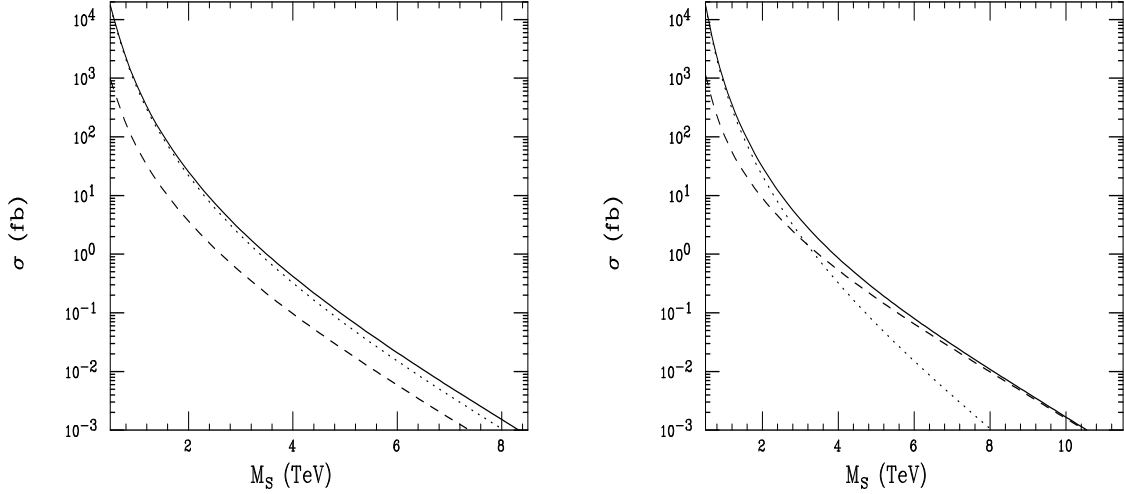
4

Figure 1: Scalar leptoquark pair production cross section as a function of mass at a 60 TeV pp(left) or $p\bar{p}$(right) LSGNA collider. The dotted(dashed) curve corresponds to the $gg(q\bar{q})$ production subprocess whereas the solid curve is their sum. MRSA$'$ parton densities are employed (from Ref. [15]).
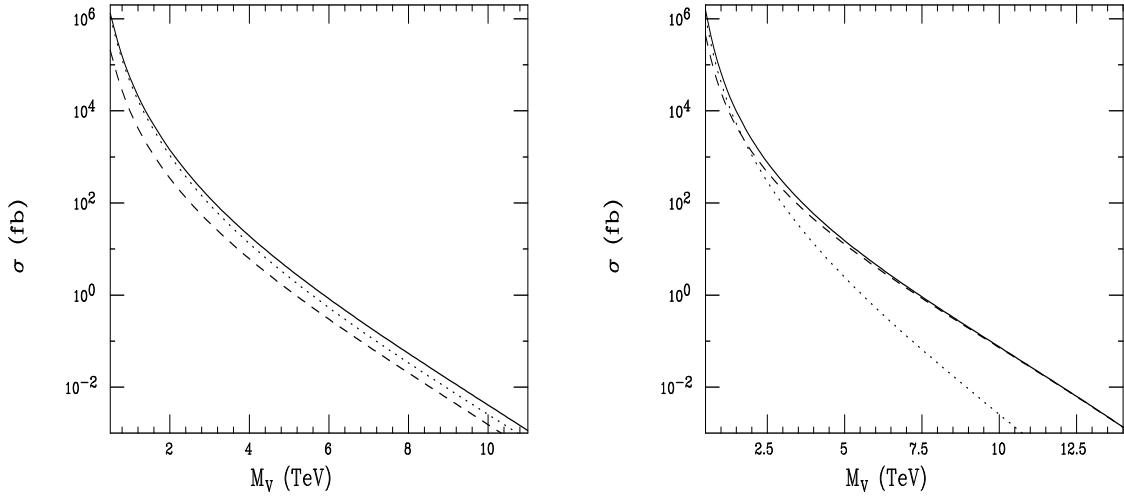

Figure 2: Same as the previous figure but now for a spin-1 vector leptoquark with $\kappa = 1$ (from Ref. [15]).

- Due to the contribution of the $q\bar{q}$ production mode, $p\bar{p}$ colliders have larger leptoquark cross sections than do pp colliders.

- At pp machines, for both vector and scalar leptoquarks, the cross sections are dominated by the gg process out to the machine's anticipated mass reach.

- In the $\sqrt{s} = 60$ TeV $p\bar{p}$ case, the $q\bar{q}$ process dominates over gg for masses greater than about 3.0(1.8) TeV for scalar(vector) leptoquarks. In the $\sqrt{s} = 200$ TeV $p\bar{p}$ case, the $q\bar{q}$ process dominates over gg for masses greater than about 10(6) TeV for scalar(vector) leptoquarks.
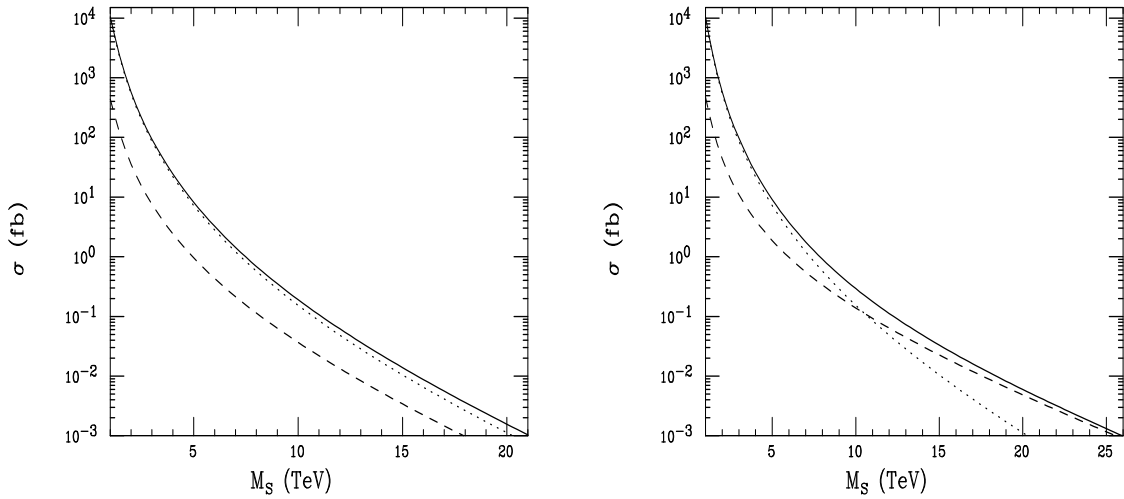

Figure 3: Same as Fig.1 but now at the 200 TeV PIPETRON collider (from Ref. [15]).

Table 1 summarizes and compares the search reaches for both scalar and vector leptoquarks at the Tevatron and LHC as well as the hypothetical 60 and 200 TeV pp and $p\bar{p}$ colliders. Rizzo's results for the Tevatron confirm the expectations of the TeV2000 Study Group [18], who also assume the 10 event discovery limit, while those obtained for the LHC are somewhat smaller[19] than that given by the fast CMS detector simulation described in the next section.
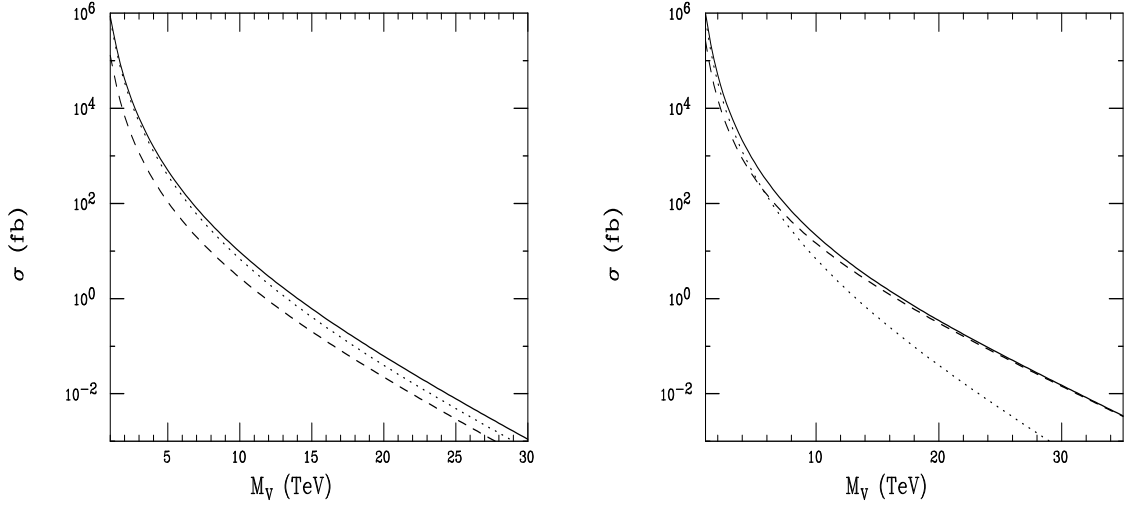
6

Figure 4: Same as Fig.2 but now for the 200 TeV PIPETRON collider (from Ref. [15]).

Machine	$\mathcal{L}(fb^{-1})$	S	V
LHC	100	1.34(1.27)	2.1(2.0)
60 TeV(pp)	100	4.9(4.4)	7.6(7.0)
60 TeV$(p\bar{p})$	100	5.7(5.2)	9.6(9.0)
200 TeV(pp)	1000	15.4(14.1)	24.2(23.3)
200 TeV$(p\bar{p})$	1000	18.1(16.2)	31.1(29.0)
TeV33	30	$\simeq 0.35$	$\simeq 0.58$

Table 1: Search reaches in TeV for scalar(S) and vector(V) leptoquarks at future hadron colliders assuming a branching fraction into a charged lepton plus a jet of unity(1/2). For vector leptoquarks, $\kappa = 1$ has been assumed and in both cases the MRSA$'$ parton densities have been employed. These results are based on the assumption of 10 signal events (from Ref. [15]).

4 Pair Production of Leptoquarks in the CMS Detector

Wrochna[19] carried out a study of the ability of the CMS detector to discover a second generation leptoquark using its muon-jet decay. The CMS detector was simulated using the package CMSJET[20]. The leptoquark, being a heavy particle, gives rise to harder muon and jet spectrums than the Standard Model backgrounds. Therefore a cut on the transverse momenta of the muons drastically reduces the background. Other cuts to isolate the signal are discussed in Ref. [19].

The signal and background after imposition of all the kinematic and topological cuts is shown in Fig. 5 for 100 fb^{-1} of luminosity. The reach of the CMS detector in leptoquark mass is about 1.6 TeV, at which point the number of signal events becomes marginal.
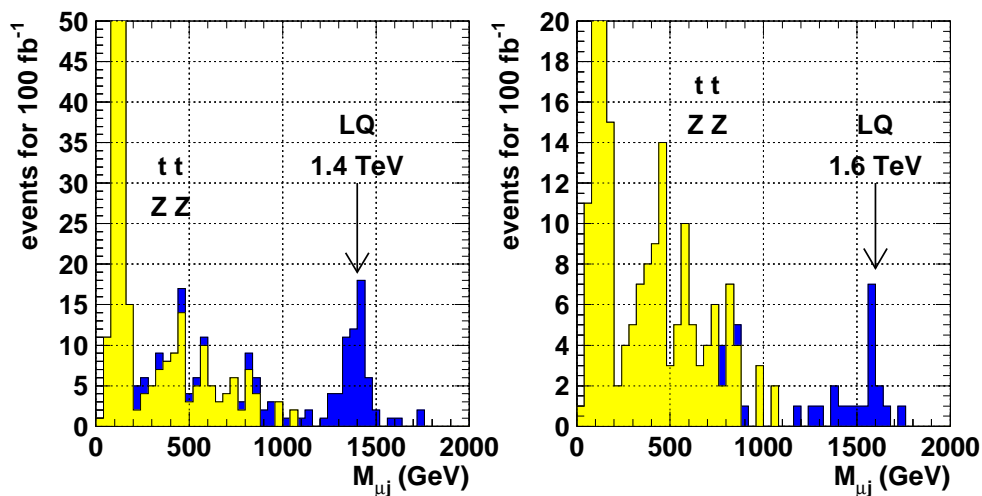

Figure 5: Leptoquark signal and background mass distribution in the CMS detector (from Ref. [19]).

5 Single Leptoquark Production at Lepton Colliders

Leptoquark production and identification was studied for lepton colliders by Doncheski and Godfrey[21]. The production modes often considered are pair production for e^+e^- and $\mu^+\mu^-$ machines. Single leptoquark production can be arise for the $e\gamma$ mode (A muon beam cannot be converted into a photon beam for kinematic reasons[22].). Leptoquarks can be produced singly in the $e\gamma$ mode, so higher masses can be probed than in double leptoquark production. e^+e^- scattering. Furthermore single leptoquark production can take place at e^+e^- and $\mu^+\mu^-$ machines by considering Weisacker-Williams photons inside the incident leptons. The production cross section depends on an unknown Yukawa coupling g; in the contribution of Doncheski and Godfrey this coupling is chosen to be equal to the electromagnetic coupling, i.e. $g^2/4\pi = \alpha_{em}$. One can also use polarization and angular distributions to determine the properties of the leptoquarks. One useful observable that has been defined[23] to isolate the spin of a leptoquark is the double asymmetry

$$A_{LL} = \frac{(\sigma^{++} + \sigma^{--}) - (\sigma^{+-} + \sigma^{-+})}{(\sigma^{++} + \sigma^{--}) + (\sigma^{+-} + \sigma^{-+})} \ , \tag{2}$$

where the first index is the final state electron helicity and the second index is the final state quark helicity. Scalar leptoquarks only contribute when the electron and quark helicities are the same, and vector leptoquarks only contribute when they are opposite. Therefore at the *parton* level one has the asymmetry $\hat{a}_{LL} = \pm 1$ for scalars and vectors, and one expects this division to survive the folding in of the parton distribution functions.

A second observable for identifying leptoquarks is the left-right asymmetry, defined as

$$A^{+-} = \frac{\sigma^+ - \sigma^-}{\sigma^+ + \sigma^-} = \frac{C_L^2 - C_R^2}{C_L^2 + C_R^2} \ . \tag{3}$$

This measurement can be used to determine the chirality of the leptoquark coupling.

The high energy photon is obtained in one of two ways: (1) as a Weisacker-Williams photon, or more optimistically (2) as a backscattered laser photon. The resulting photon is then resolved into its hadronic content as shown in Fig. 6 and single leptoquark production can result. The backscattered photon gives a slightly

reduced maximum center-of-mass energy than does a Weisacker-Williams photon, but it gives a harder photon spectrum with higher luminosity, but requires including the backscattering option in the collider design. The cross sections for single leptoquark production are shown in Figs. 7 and 8. The cross section is significantly higher for the backscattered photon, but the ultimate reach in energy is slightly less.
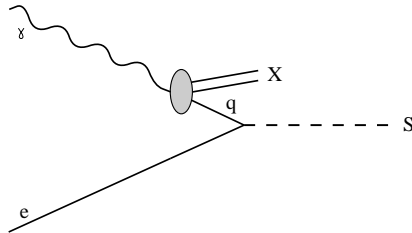

Figure 6: The resolved photon contribution for leptoquark production in $e\gamma$ collisions (from Ref. [21]).
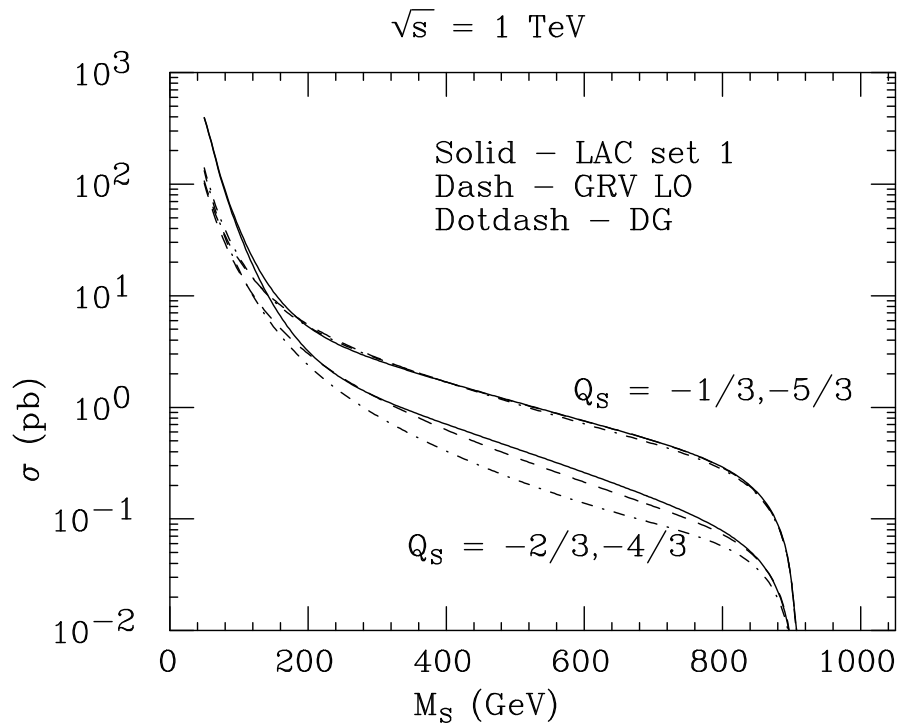

Figure 7: The cross sections for leptoquark production due to resolved photon contributions in $e\gamma$ collisions for laser backscattered photons at a $\sqrt{s} = 1\ TeV$ collider. The solid, dashed, dot-dashed lines are for resolved photon distribution functions LAC, GRV and DG respectively (from Ref. [21]).
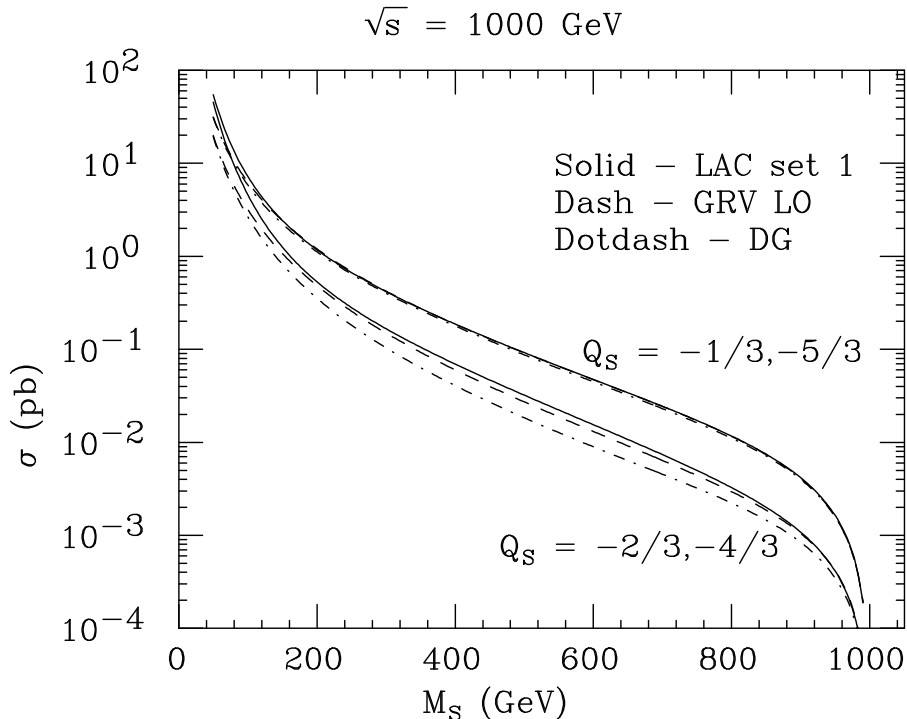
10

Figure 8: The cross sections for leptoquark production due to resolved photon contributions in $e\gamma$ collisions for Weizsäcker-Williams photons at a $\sqrt{s} = 1\,TeV$ collider. The solid, dashed, dot-dashed lines are for resolved photon distribution functions LAC, GRV and DG respectively (from Ref. [21]).

For colliders with a center-of-mass energies above 1 TeV, the reach for single leptoquark production in this process is essentially the kinematic limit provided the planned luminosities of the machines is indeed realized. For a $\sqrt{s} = 500$ GeV machine there are some small differences between e^+e^- machines and $\mu^+\mu^-$ machines: there are larger u and d content in the photon because their mass is smaller, so an e^+e^- collider have a 25% higher reach than a $\mu^+\mu^-$ collider at the same energy. However, it should be remembered that the two machines are probing different leptoquarks (first-generation versus second-generation), so that the searches are actually complementary. The discovery limits obtained by Donchecki and Godfrey[21] are given in Table 2.

6 Indirect Searches for Leptoquarks

At $e^+ e^-$ and $\mu^+ \mu^-$ colliders, pairs of leptoquarks can be produced directly via the s-channel γ and Z exchange. The reach for the leptoquark mass for this mode is essentially the kinematic limit, i.e. $M_S < \sqrt{s}/2$. However even if a leptoquark is too massive to be produced directly, it can contribute[7, 24, 25] indirectly to the process $\ell^+ \ell^- \to q\bar{q}$ by interfering with the Standard Model diagrams as shown in Fig. 9. The leptoquark interacts via a Yukawa coupling which can be parametrized in the form

$$\mathcal{L} \;\; = \;\; gS\bar{q}(\lambda_L P_L + \lambda_R P_R)\ell \; , \tag{4}$$

where g is the weak coupling constant (to set the overall magnitude of the interaction) and $\lambda_{L,R}$ are dimensionless constants. P_L and P_R are the left- and right-handed projectors. The amplitudes for the diagrams presented in Fig. 9 have been presented for the unpolarized case in Ref. [7], and is generalized to the case with polarization in Ref. [25]. The size of the interference effect is determined by the three parameters M_S, λ_L and λ_R.

By examining the overall rate and the angular distribution, indirect evidence for leptoquarks can be obtained. Berger[26] examined the bounds which can be placed on the leptoquark mass including the option of polarizing the electron and muon beams. The polarization of the beams of a lepton collider can serve two purposes in indirect leptoquark searches: (1) it can extend the reach of the indirect search by serving to enhance the fraction of initial leptons to which the leptoquark couples; (2) it can measure the left-handed and right-handed couplings of the leptoquark separately.
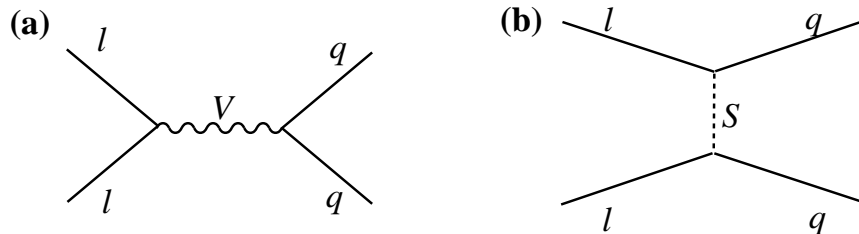
Figure 9: The Feynman diagrams for the process $\ell^+ \ell^- \to q\bar{q}$ include the (a) Standard Model diagrams involving s-channel $V = \gamma, Z$ exchange, and (b) the hypothetical t-channel leptoquark S exchange (from Ref. [26]).

The deviations from the Standard Model appear in the total cross section and the angular distribution of the produced quarks[7]. The total cross section and the forward-backward asymmetry, A_{FB}, amount to integrating this distribution in one

or two bins respectively. The statistical significance of the signal is determined by calculating a χ^2 for the deviation from the expectation in the Standard Model[25],

$$\chi^2 = \sum_{j=1}^{18} \frac{(n_j^{\mathrm{LQ}} - n_j^{\mathrm{SM}})^2}{n_j^{\mathrm{SM}}} , \qquad (5)$$

where n_j^{SM} is the number of events expected in each $\Delta \cos\theta = 0.1$ bin in the Standard Model, and n_j^{LQ} is the number of events including the leptoquark.

The additional piece in the Lagrangian that is of relevance to us can be parametrized in the form

$$\mathcal{L} = gS\bar{q}(\lambda_L P_L + \lambda_R P_R)\ell , \qquad (6)$$

where g is the weak coupling constant (to set the overall magnitude of the interaction) and $\lambda_{L,R}$ are dimensionless constants. P_L and P_R are the left- and right-handed projectors. The size of the interference effect will be determined by the three parameters M_S, λ_L and λ_R.

Figure 10 shows the 95% c.l. bounds that could be achieved on a leptoquark with right-handed couplings ($\lambda_L = 0$) at a $\sqrt{s} = 4$ TeV e^+e^- collider, with nonpolarized beams and with 80% and 100% polarization of the electron beam. We have assumed integrated luminosity L_0 and efficiency ϵ for detecting the final state quarks so that $\epsilon L_0 = 70\mathrm{fb}^{-1}$. Polarization from 80% to 100% roughly brackets the range that might reasonably be achievable for the electron beam. Figure 11 shows the same bounds for the case where the leptoquark has left-handed couplings ($\lambda_R = 0$).

In a muon collider both μ^+ and μ^- beams can be at least partially polarized, but perhaps with some loss of luminosity[27]. If one tolerates a drop in luminosity of a factor two, then one can achieve polarization of both beams at the level of $P^- = P^+ = 34\%$. It might be possible to maintain the luminosity at its full unpolarized value if the proton source intensity (a proton beam is used to create pions that decay into muons for the collider) could be increased[27]. Results for each of these three possible scenarios below in Fig. 12 for a leptoquark with right-handed couplings and in Fig. 13 for a leptoquark with left-handed couplings. In the former case polarization is useful for improving the leptoquark bounds even with a loss of two in luminosity.
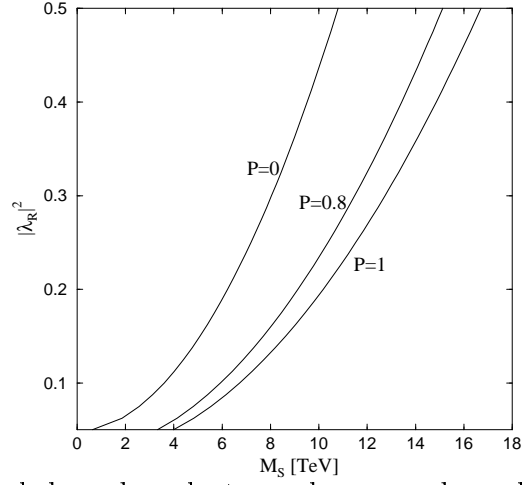
13

Figure 10: The 95% c.l. bounds on leptoquark mass and couplings at a $\sqrt{s} = 4$ TeV e^+e^- collider for a leptoquark with right-handed couplings only ($\lambda_L = 0$). The electron polarization P is set to 0%, 80% and 100%, and the positron is always unpolarized. The area above each curve would be excluded (from Ref. [26]).
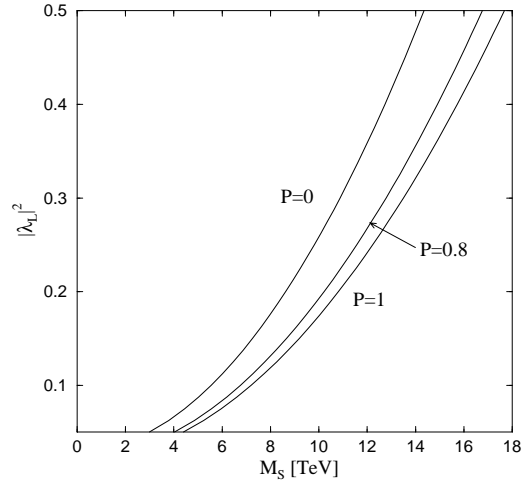

Figure 11: The 95% c.l. bounds on leptoquark mass and couplings at a $\sqrt{s} = 4$ TeV e^+e^- collider for a leptoquark with left-handed couplings only ($\lambda_R = 0$). The electron polarization P is set to 0%, 80% and 100%, and the positron is always unpolarized. The area above each curve would be excluded (from Ref. [26]).
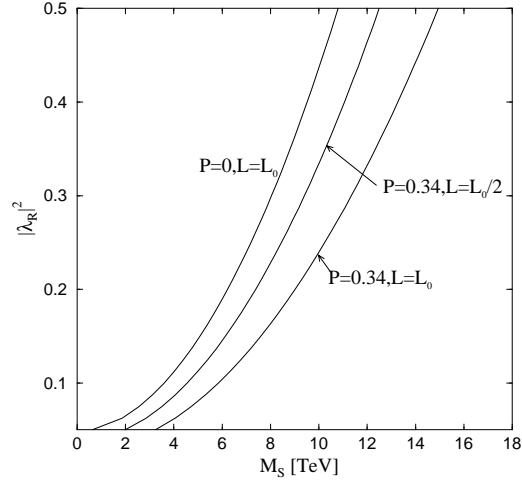
14

Figure 12: The 95% c.l. bounds on leptoquark mass and couplings at a $\sqrt{s} = 4$ TeV $\mu^+\mu^-$ collider for a leptoquark with right-handed couplings only ($\lambda_L = 0$). The curves indicate the bounds for nonpolarized beams, both μ^+ and μ^- having polarization P is set to 34% and no reduction in luminosity, and both μ^+ and μ^- having polarization P is set to 34% and a reduction in luminosity of a factor of two. The area above each curve would be excluded (from Ref. [26]).

Figure 13: The 95% c.l. bounds on leptoquark mass and couplings at a $\sqrt{s} = 4$ TeV $\mu^+\mu^-$ collider for a leptoquark with left-handed couplings only ($\lambda_R = 0$). The curves indicate the bounds for nonpolarized beams, both μ^+ and μ^- having polarization P is set to 34% and no reduction in luminosity, and both μ^+ and μ^- having polarization P is set to 34% and a reduction in luminosity of a factor of two. The area above each curve would be excluded (from Ref. [26]).
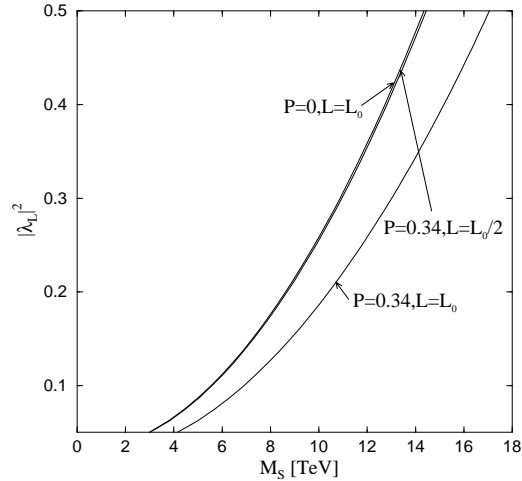
One can compare the utility of polarizing both beams as opposed to polarizing just one beam. This can be done by comparing Figs. 10 and 12 for the right-handed leptoquark case and Figs. 11 and 13 for the left-handed leptoquark case. The bounds for leptoquarks with interactions of order the weak coupling strength are summarized in Table III, for both left-handed couplings ($|\lambda_L|^2 = 0.5, |\lambda_R|^2 = 0$) and right-handed couplings ($|\lambda_R|^2 = 0.5, |\lambda_L|^2 = 0$). For both cases one sees that the 34% polarization of both beams gives roughly the same bounds as a collider with one beam polarized at the 80-90% level.

7 Bilepton Searches at the NLC

A new particle which couples to two Standard Model leptons has been named a bilepton, and sometimes has been called a dilepton. Cuypers and Davidson[28] have studied the discovery prospects for the NLC. They study all of the possible NLC modes, e^+e^-, e^-e^-, $e^-\gamma$ and $\gamma\gamma$. For their study they assumed a luminosity which scales with energy as

$$\mathcal{L}[\text{fb}^{-1}] = 200s[\text{TeV}^2] , \tag{7}$$

in the e^+e^- mode. For the e^-e^- mode, they assume the luminosity is reduced by a factor of two compared to the e^+e^- mode.

The quantum numbers and couplings of the bileptons is shown in Table 4. The numerical index indicates bileptons which are singlets, doublets or triplets under the weak SU(2) gauge symmetry, and vector bileptons also carry an index μ. Bileptons carry either zero total lepton number (and some of the Standard Model particles fall into this category), or carry two units of lepton number. See Ref. [28] for more details about their interactions.

If the NLC is operated in the e^-e^- mode, it can produce doubly charged bileptons in the s-channel. The signal is a pair of like-sign leptons; flavor violating processes like $e^-e^- \to \mu^-\mu^-$ might even be possible. IF one knows the mass of the new particle, one could try to set the center of mass energy so as to sit on the resonance. If the leptonic couplings are small, it is possible that the signal will be reduced because the bilepton width is even smaller than the beam energy spread. Cuypers and Davidson find the the 95% c.l. lower limits on the bilepton masses are of the order of

$$m_L \gtrsim \sqrt{s} \times 50\lambda_{ee} , \tag{8}$$

16

where λ_{ee} is the coupling of the bilepton to $e^- e^-$.

Singly-charged bileptons can be produced in $e^- \gamma$ scattering, but there is no resonance in this case. Figure 14 shows the discovery potential found by Cuypers and Davidson of $e^- \gamma$ collisions for several center of mass energies.

Singly-charged bileptons can also be pair produced in $e^+ e^-$ collisions. In Fig. 15 the number of expected bilepton events is shown for right-polarized $e^+ e^-$ collisions (the beams are polarized to eliminate Standard Model backgrounds). A viable signal is obtained all the way to the kinematic limit.

Above the kinematic limit ($m_L > \sqrt{s}/2$), the bileptons can have an indirect effect on Bhahba scattering and produce significant deviations from the Standard Model predictions (this is analoqous to the indirect effects of leptoquarks described in the previous section). Cuypers and Davidson again find the 95% C.L. lower limits on the bilepton masses are of the order of

$$m_L \gtrsim \sqrt{s} \times 50 \lambda_{ee} \ . \tag{9}$$

8   Neutral Heavy Leptons

Kalyniak and Melo[29] have studied the production of a single neutral heavy lepton (NHL) in association with a massless neutrino in $e^+ e^-$ and $\mu^+ \mu^-$ colliders[30, 31, 32]. The models considered have two new weak isosignlet neutrino fields per generation yielding three massless neutrinos (ν_i) and three Dirac NHL's (N_a)[33, 34, 35, 36]. The Feynman diagrams are shown in Fig. 16. The weak interaction eigenstates, $\nu_\ell, \ell = e, \mu, \tau$, are related to the neutrino mass eignestates via two 3×3 mixing matrices:

$$\nu_\ell \ = \ \sum_{i=1,2,3} (K_L)_{li} \nu_{iL} + \sum_{i=4,5,6} (K_K)_{la} N_{aL} \tag{10}$$

The cross sections are characterized by the mass of the heavy lepton M_N and the mixing parameters

$$\ell\ell_{mix} \ = \ \sum_{a=4,5,6} (K_H)_{la} (K_H^\dagger)_{al} \ , \tag{11}$$

for $\ell = e, \mu, \tau$. The existing constraints on the mixings are[37]

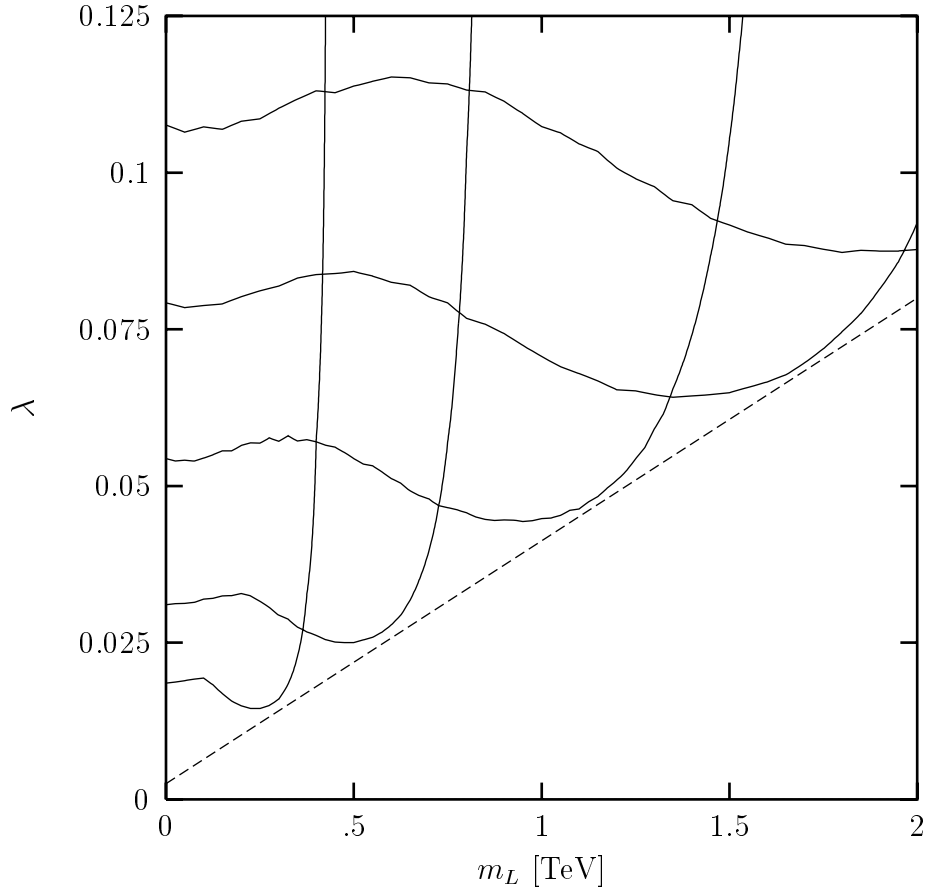$$ee_{mix} \ \leq \ \ 0.0071 \ , \tag{12}$$

17

Figure 14: Smallest observable scalar bilepton L_1^- couplings to leptons at the one standard deviation level as a function of the bilepton mass and coupling in $e^-\gamma$ collisions. The collider's e^+e^- center of mass energies are .5, 1, 2, and 3 TeV from left to right (from Ref. [28]).

$$\mu\mu_{mix} \leq \quad 0.0014 \, , \tag{13}$$

$$\tau\tau_{mix} \leq \quad 0.033 \, . \tag{14}$$

Since the best bound occurs for the second generation, the largest possible effects that are still allowed occur at an e^+e^- collider. The cross section depends on various mixing parameters[29]:

$$t_{mix} \quad = \quad |(K_L^*)_{li}(K_H)_{la}|^2 \, , \tag{15}$$

$$s_{mix} \quad = \quad |(K_L^\dagger K_H)_{ia}|^2 \, , \tag{16}$$

$$st_{mix} \quad = \quad (K_L^\dagger K_H)_{ia}(K_L)_{li}(K_H^*)_{la} \, , \tag{17}$$

18
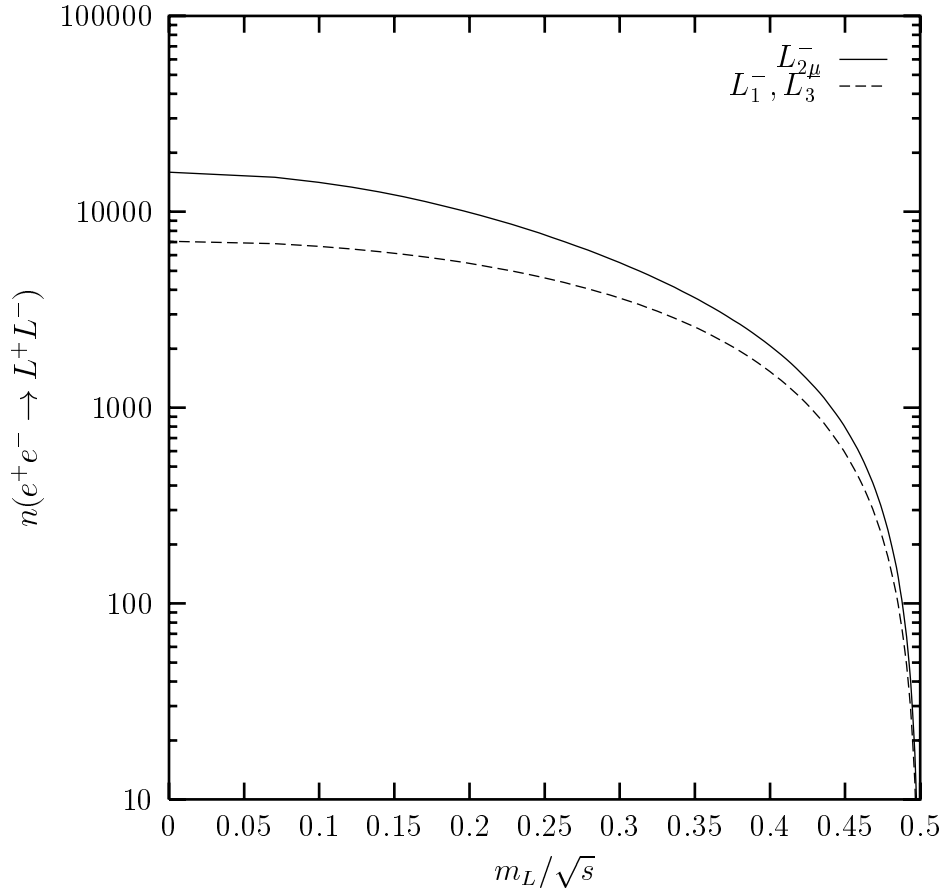
Figure 15: Mass dependence of the number of pair-produced singly-charged bileptons in e^+e^- annihilations (from Ref. [28]).

which are bounded by the constraints listed above.

The single NHL production cross sections are displayed as a function of M_N in Fig. 17 for $\sqrt{s} = 0.5, 1.0, 1.5$ TeV e^+e^- colliders and for $\sqrt{s} = 0.5$ TeV $\mu^+\mu^-$ colliders. The maximal signal is smaller for muon colliders because of the tighter constraint on $\mu\mu_{mix}$ relative to ee_{mix}. In Fig. 18 the single NHL production cross sections are displayed for a $\sqrt{s} = 5$ TeV e^+e^- collider and for a $\sqrt{s} = 4$ TeV $\mu^+\mu^-$ collider.
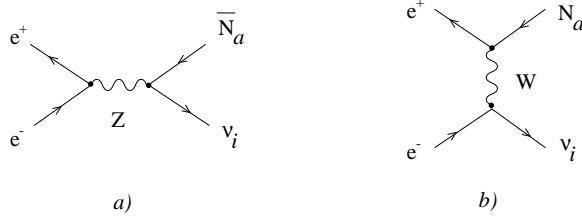
Figure 16: Feynman diagrams for $e^+e^- \rightarrow \overline{N_a}\nu_i$ in the (a) s-channel and the (b) t-channel (from Ref. [29]).

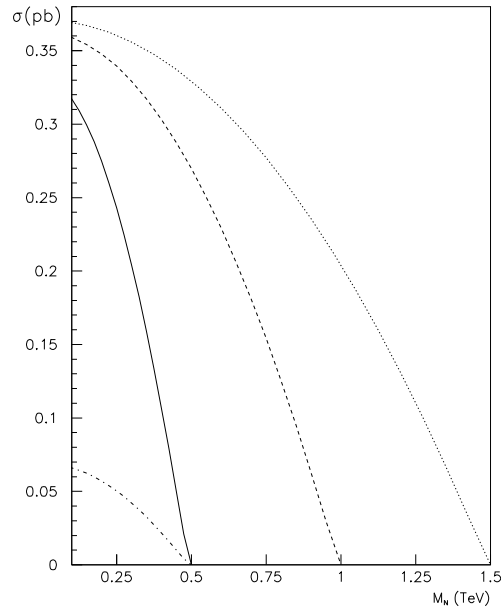Figure 17: Total cross section versus NHL mass M_N for an e^+e^- collider at three different energies: $\sqrt{s} = 0.5$ TeV (solid line), $\sqrt{s} = 1.0$ TeV (dashed line) and $\sqrt{s} = 1.5$ TeV (dotted line), and for a $\mu^+\mu^-$ collider at $\sqrt{s} = 0.5$ TeV (dash-dotted line) (from Ref. [29]).
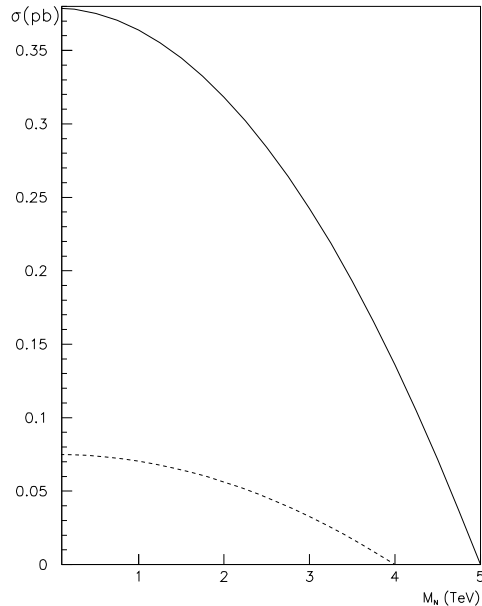
Figure 18: Total cross section versus NHL mass M_N for an e^+e^- collider at $\sqrt{s} =$ 5.0 TeV (solid line) , and for a $\mu^+\mu^-$ collider at $\sqrt{s} = 4.0$ TeV (dashed line) (from Ref. [29]).

The discovery limits for NHL masses and mixings for the special case $t_{mix} = s_{mix} = st_{mix}$ is shown in Table V for the various machines and integrated luminosities. The higher energy machines will be sensitive to mixings in the 10^{-5} to 10^{-6} range for much of the range of M_N.

9   Conclusions

The New Particles Subgroup concentrated on leptoquark signals at present and future colliders. The prospects for identifying the particle by measuring its properties was also addressed. Search strategies for bileptons at the NLC and neutral heavy leptons at electron and muon colliders were described.

The signals for detection of these particles falls into three classes: direct detection by (1) single production or (2) pair production, or indirect detection through their

virtual effects. Whether or not any of these new particles exists in nature is an open question, but the new colliders under study at the Snowmass workshop will certainly extend the range far beyond the existing limits.

Acknowledgement

REFERENCES

1. K. Cheung and R.M. Harris, these proceedings, hep-ph/9610382.

2. A. Djouadi, J. Ng and T.G. Rizzo, SLAC-PUB-95-6772, 1995, a part of the DPF long-range planning study to be published in *Electroweak Symmetry Breaking and Physics Beyond the Standard Model*, eds. T. Barklow, S. Dawson, H. Haber, and J. Seigrist (World Scientific 1996), hep-ph/9504210.

3. P. Langacker, Phys. Rep. **72**, 185 (1981); J.L. Hewett and T.G. Rizzo, Phys. Rep. **183**, 193 (1989).

4. H. Georgi and S.L. Glashow, Phys. Rev. Lett. **32**, 438 (19744).

5. J.L. Hewett and S. Pakvasa, Phys. Rev. **D37**, 3165 (1988); O.J.P. Éboli and A.V. Olinto, Phys. Rev. **D38**, 3461 (1988); J. Ohnemus, et al., Phys. Lett. **B334**, 203 (1994).

6. J. Wudka, Phys. Lett. **B167**, 337 (1986); M.A. Doncheski and J.L. Hewett, Z. Phys. **C56**, 209 (1992); J. Blümlein, E. Boos, and A. Pukhov, Int. J. Mod. Phys. **A9**, 3007 (1994).

7. J.L. Hewett and T.G. Rizzo, Phys. Rev. **D36**, 3367 (1987).

8. J.L. Hewett and S. Pakvasa Phys. Lett. **B227**, 178 (1987); J.E. Cieza and O.J.P. Éboli, Phys. Rev. **D47**, 837 (1993); J. Blümein and R. Rückl, Phys. Lett. **B304**, 337 (1993); J. Blümlein and E. Boos, Nucl. Phys. **B37** (Proc. Suppl.),181 (1994).

9. O.J.P. Éboli *et al.*, Phys. Lett. **B311**, 147 (1993); H. Nadeau and D. London, Phys. Rev. **D47**, 3742 (1993); M.A. Doncheski and S. Godfrey, Phys. Rev. **D51** (1995) 1040.

10. G. Bélanger, D. London, and H. Nadeau, Phys. Rev. **D49**, 3140 (1994).

11. P. Maettig, OPAL Collaboration, talk given at the *28th International Conference on High Energy Physics*, Warsaw, Poland, 25-31 July 1996.

12. S. Aid *et al.*, H1 Collaboration, Phys. Lett. **B369**, 173 (1996); D. Krakauer, ZEUS Collaboration, these proceedings.

13. S. Abachi *et al.*, D0 Collaboration, Phys. Rev. Lett. **75**, 3618 (1995) and Phys. Rev. Lett. **72**, 965 (1994); F. Abe *et al.*, CDF Collaboration, Phys. Rev. Lett. **75**, 1012 (1995) and Phys. Rev. **D48**, 3939 (1993); H. Wenzel, CDF Collaboration, talk given at the *XI Topical Workshop on $p\bar{p}$ Collider Physics*, Padova, Italy, 27 May-1 June, 1996.

14. S. Davidson, D. Bailey, and B.A. Campbell, Z. Phys. **C61**, 613 (1994); M. Leurer, Phys. Rev. **D49**, 333 (1994) and Phys. Rev. **D50**, 536 (1994); W. Buchmüller, and D. Wyler, Phys. Lett. **B177**, 377 (1986).

15. T. Rizzo, these proceedings, hep-ph/9609267.

16. J.L. Hewett and S. Pakvasa, Phys. Rev. **D37**, 3165 (1988).

17. J.E. Cieza Montalvo and O. Eboli, Phys. Rev. **D47**, 837 (1993); J. Blümlein and R. Rückl, Phys. Lett. **B304**, 337 (1993); J.L. Hewett, T.G. Rizzo, S. Pakvasa, A. Pomarol, and H.E. Haber, in the *Proceedings of the Workshop on Physics at Current Accelerators and Supercolliders*, edited by J. Hewett, A. White and D. Zeppenfeld, Argonne National Laboratory, 2-5 June, 1993.

18. See the discussion in *Future ElectroWeak Physics at the Fermilab Tevatron: Report of the tev_{2000} Study Group*, eds. D. Amidei and R. Brock, D0 Note 2589 and CDF Note 3177, 1996.

19. G. Wrochna, these proceedings.

20. S. Abdulin, A. Khanov, N. Stepanov, CMS Technical Note CMS TN/94-180.

21. M. Doncheski and S. Godfrey, these proceedings.

22. V. Barger, M.S. Berger, J.F. Gunion and T. Han, *Particle Physics Opportunities at $\mu^+\mu^-$ Colliders*, MADPH-96-939, hep-ph/9604334.

23. M.A. Doncheski and S. Godfrey, Phys. Rev. **D51**, 1040 (1995).

24. H. Dreiner, et al., Mod. Phys. Lett. **A3**, 443 (1988).

25. D. Choudhury, Phys. Lett. **B346**, 291 (1995).

26. M.S. Berger, these proceedings, hep-ph/9609517.

27. $\mu^+\mu^-$ Collider: A Feasibility Study, BNL-52503, July 1996.

28. F. Cuypers and S. Davidson, PSI-PR-96-21, hep-ph/9609487; and these proceedings.

29. P. Kalyniak and I. Melo, these proceedings.

30. W. Buchmüller et al., in *Proceedings of the Workshop on e^+e^- Collisions at 500 GeV: The Physics Potential,* p. 539, DESY 92-123B (1992).

31. G. Azuelos and A. Djouadi, Z. Phys. **C63**, 327 (1994).

32. J. Maalampi, K. Mursula and R. Vuopionperä, Nucl. Phys. **B372**, 23 (1991).

33. G. Bhattacharya, P. Kalyniak and I. Melo, Phys. Dev. **D51**, 3569 (1995).

34. R.N. Mohapatra and J.W.F. Valle, Phys. Rev. **D34**, 1642 (1986).

35. J. Bernabéu, A. Santamaria, J. Vidal, A. Mendez and J.W.F. Valle, Phys. Lett. **B187**, 303 (1987).

36. D. Wyler and L. Wolfenstein, Nucl. Phys. **B218**, 205 (1983).

37. E. Nardi, E. Roulet and D. Tammasins, Phys. Lett. **B327**, 319 (1994).

e^+e^- Colliders					
$\sqrt{s}$ (TeV)	$L(fb^{-1})$	Scalar		Vector	
		-1/3, -5/3	-4/3, -2/3	-1/3, -5/3	-4/3, -2/3
0.5	50	490	470	490	480
1.0	200	980	940	980	970
1.5	200	1440	1340	1470	1410
5.0	1000	4700	4200	4800	4500

$e\gamma$ Colliders					
$\sqrt{s}$ (TeV)	$L(fb^{-1})$	Scalar		Vector	
		-1/3, -5/3	-4/3, -2/3	-1/3, -5/3	-4/3, -2/3
0.5	50	450	450	450	440
1.0	200	900	900	910	910
1.5	200	1360	1360	1360	1360
5.0	1000	4500	4400	4500	4500

$\mu^+\mu^-$ Colliders					
$\sqrt{s}$ (TeV)	$L(fb^{-1})$	Scalar		Vector	
		-1/3, -5/3	-4/3, -2/3	-1/3, -5/3	-4/3, -2/3
0.5	0.7	250	170	310	220
0.5	50	400	310	440	360
5.0	1000	3600	3000	3700	3400

Table 2: Search reaches in TeV for scalar(S) and vector(V) leptoquarks at future hadron colliders assuming a branching fraction into a charged lepton plus a jet of unity(1/2). For vector leptoquarks, couplings of electromagnetic strength have been assumed and in both cases the MRSA$'$ parton densities have been employed. These results are based on the assumption of 10 signal events (from Ref. [21]).

Table 3: Bounds on leptoquark masses at 98.6% confidence level, assuming either left-handed couplings ($|\lambda_L|^2 = 0.5, |\lambda_R|^2 = 0$) or right-handed couplings ($|\lambda_L|^2 = 0, |\lambda_R|^2 = 0.5$) (from Ref. [26]).

Luminosity and Polarization(ℓ^-, ℓ^+)	Coupling	M_S-Bound (TeV)
L_0 (0%,0%)	Left	14.3
	Right	10.8
L_0 (80%,0%)	Left	16.8
	Right	15.1
L_0 (100%,0%)	Left	17.7
	Right	16.7
L_0 (34%,34%)	Left	17.1
	Right	14.9
$L_0/2$ (34%,34%)	Left	14.4
	Right	12.5

	L	J	Y	T_3	Q_γ	Q_Z	lepton couplings	familiar sibling
L_1^μ	0	1	0	0	0	0	$\bar{e}_L e_L\ (g_1)$ $\nu_L\nu_L\ (g_1)$	γ Z^0 Z'
$\tilde{L}_1^\mu$	0	1	0	0	0	0	$\bar{e}_R e_R\ (\tilde{g}_1)$	γ Z^0 Z'
L_2	0	0	1/2	1/2	1	$-\dfrac{2\sin^2\theta_w-1}{2\sin\theta_w\cos\theta_w}$	$\bar\nu_L e_R\ (g_2)$	H^+
				$-1/2$	0	$-\dfrac{1}{2\sin\theta_w\cos\theta_w}$	$\bar{e}_L e_R\ (g_2)$	H
L_3^μ	0	1	0	1	1	$\dfrac{\cos\theta_w}{\sin\theta_w}$	$\bar\nu_L e_L\ (\sqrt{2}g_3)$	W^+ W'^+
				0	0	0	$e_L e_L\ (-g_3)$ $\bar\nu_L\nu_L\ (g_3)$	γ Z^0 Z'
				-1	-1	$-\dfrac{\cos\theta_w}{\sin\theta_w}$	$\bar{e}_L\nu_L\ (\sqrt{2}g_3)$	W^- W'^-
L_1	2	0	1	0	1	$-\dfrac{\sin\theta_w}{\cos\theta_w}$	$e_L\nu_L\ (\lambda_1)$ (antisymm.)	
$\tilde{L}_1$	2	0	2	0	2	$-2\dfrac{\sin\theta_w}{\cos\theta_w}$	$e_R e_R\ (\tilde\lambda_1)$ (symm.)	
L_2^μ	2	1	3/2	1/2	2	$-\dfrac{4\sin^2\theta_w-1}{2\sin\theta_w\cos\theta_w}$	$e_R e_L\ (\lambda_2)$	
				$-1/2$	1	$-\dfrac{2\sin^2\theta_w+1}{2\sin\theta_w\cos\theta_w}$	$e_R\nu_L\ (\lambda_2)$	
L_3	2	0	1	1	2	$-\dfrac{2\sin^2\theta_w-1}{\sin\theta_w\cos\theta_w}$	$e_L e_L\ (\sqrt{2}\lambda_3)$	
				0	1	$-\dfrac{\sin\theta_w}{\cos\theta_w}$	$e_L\nu_L\ (\lambda_3)$ (symm.)	
				-1	0	$-\dfrac{1}{\sin\theta_w\cos\theta_w}$	$\nu_L\nu_L\ (-\sqrt{2}\lambda_3)$	

Table 4: Major quantum numbers and couplings of the bileptons (from Ref. [28]).

27

$\sqrt{s}$(TeV)	$L(fb^{-1})$	$M_N(TeV)$	t_{mix}
1.0	200	0.5	7×10^{-6}
		0.75	1×10^{-5}
		0.95	6×10^{-5}
1.5	200	0.5	5×10^{-6}
		1.0	9×10^{-6}
		1.25	2×10^{-5}
		1.45	8×10^{-5}
4.0	1000	0.5	9.5×10^{-7}
		1.0	1×10^{-6}
		2.0	1.2×10^{-6}
5.0	1000	0.5	9.4×10^{-7}
		1.0	9.5×10^{-7}
		2.0	1.1×10^{-6}

Table 5: Discovery limits for NHL masses and mixings (from Ref. [29]).